SUPPORTING INFORMATION

"Resolution of Inflammation by 17(S)-HDHA Confers Neuroprotection After Ischemic Spinal Cord Injury"

[1,2]Caio Perret[¶], [1]Tagore G. de Morais[¶], [1]Chiara D. Pimentel, [2]Raphael M. Bertani, [3]Rene O. Beleboni, [4]Fabio C.S. Nogueira, [5]Karsten Gronert, [1,6,7]Renato Rozental[*].

SI ILLUSTRATIONS:

- 2 SUPPLEMENTARY FIGURES
- 1 SUPPLEMENTARY TABLE

SUPPORTING INFORMATION
Perret et al. – Nature Spinal Cord

SI Materials and Methods

The study was conducted in accordance with applicable NIH guidelines for research involving human participants and laboratory animals and was approved by the relevant institutional ethics committees in Brazil and the United States: the Federal University of Rio de Janeiro, Brazil (CAAE 37520820.4.3001.5259; CEUA-UFRJ DAHEICB 053); Universidade de Ribeirão Preto, Brazil (CEUA-UNAERP protocol no. 008/2023); Hospital Municipal Miguel Couto, Brazil (CAAE 96263418.0.0000.5279); New York Medical College, New York, USA (IACUC approval no. 69-12-0609.1); and Albert Einstein College of Medicine, New York, USA (IACUC protocol no. 20030906).

Role of the Funders. The funders had no role in the study design; data collection, analysis, or interpretation; manuscript preparation; or the decision to submit the manuscript for publication. The study was conducted independently by the authors, who are solely responsible for the study design, data integrity, interpretation of the findings, and content of the manuscript.

Study Locations and Experimental Procedures. Experimental procedures were conducted at the academic research laboratories and animal facilities, where maximal electroshock seizure (MES) stimulation and associated animal assessments were performed.

Experimental Design, Animals, and Group Allocation. The two back-to-back manuscripts were based on an integrated experimental program involving shared cohorts of female Sprague–Dawley rats. The principal SCI investigation comprised 83 animals distributed among three groups: pregnant controls receiving subthreshold electrical stimulation (n = 20), MES-stimulated animals that did not develop paralysis (n = 24), and MES-stimulated animals that developed persistent paralysis (n = 39). The latter group was subdivided into untreated animals (n = 20) and animals treated with 17(S)-hydroxydocosahexaenoic acid [17(S)-HDHA] every other day (n = 19).

The complementary manuscripts investigated distinct but connected phases of ischemic SCI. Manuscript #1 focused on early pathophysiological changes during the first 24 h after paralysis onset, whereas Manuscript #2 extended the investigation from the 24-h time point through day 5 to characterize inflammatory resolution and neuroprotection (**Supplementary Fig. 1**). The 24-h time point provided a shared temporal reference linking early inflammatory, molecular, and histological findings to subsequent disease progression and therapeutic intervention. The overall principal SCI cohort comprised 83 animals assessed across the experimental time points, with the allocation of animals to individual procedures and analyses determined by the objectives of each manuscript.

Animals were 2–3 months old and weighed 200–250 g (Taconic Farms, Germantown, NY, USA). The principal SCI-model cohort included 140 pregnant females subjected to repeated maximal electroshock seizure (MES) stimulation, as described in Manuscript #1. An additional 20 pregnant females served as controls and underwent the same handling and electrode placement but received

subthreshold stimulation (15 V), which did not induce generalized seizures. The remaining 77 MES-stimulated animals that did not develop paralysis and one animal that developed transient paralysis but recovered hindlimb movements within 3 h of the final stimulation are reported in Manuscript #1 and are not included in the experimental cohorts described here.

Two additional cohorts comprising 27 non-pregnant female rats were used exclusively for complementary experiments in Manuscript #2. These experiments investigated SC penetration of systemically administered 17(S)-HDHA under physiological conditions (n = 9) and treatment-associated metabolic effects in the absence of SCI or MES stimulation (n = 18).

MES Stimulation and Seizure Assessment. Transauricular electrical stimulation was delivered through bilateral ear-clip electrodes connected to a constant-voltage stimulator (Grass Instruments, Model S48, Quincy, MA, USA). Animals were briefly restrained for electrode placement and subsequently stimulated while awake. Each stimulation session comprised four consecutive MES stimulations delivered at 30-s intervals. Animals underwent one session during the first experimental week, four sessions during the second week, and seven sessions during the third week.

Seizure Identification and Monitoring. Generalized tonic–clonic seizures were identified by the characteristic behavioral sequence elicited by MES stimulation: tonic flexion, tonic hindlimb extension (THE; bilateral hindlimb extension to approximately 180° relative to the longitudinal body axis), generalized clonic convulsions, and postictal depression. Complete THE or tonic flexion was used as the primary behavioral criterion for successful seizure induction. Animals were continuously monitored during each stimulation session and until spontaneous locomotor activity recovered, after which they were returned to their home cages. Details of transauricular current and impedance measurements are provided in Manuscript #1.

Inclusion and Exclusion Criteria. Inclusion in the persistent-paralysis cohort required paralysis that persisted following MES stimulation. Of the 40 animals initially identified as paralyzed, one recovered hindlimb movements within 3 h of the final stimulation and was excluded from subsequent sampling and analysis in this study because the recovery did not meet the criterion for persistent paralysis. The remaining 39 animals were retained for the planned analyses.

Among the 100 pregnant MES-stimulated animals that did not develop persistent paralysis, MES-associated pregnancy termination occurred in eight animals. These animals were removed from the study and euthanized in accordance with the approved animal-welfare protocol; they were excluded from subsequent analyses. Animal numbers contributing to individual outcomes are reported in the corresponding Results sections.

Randomization and Blinding. Within the relevant experimental groups, animals were randomly selected for electromyographic, magnetic resonance imaging (MRI), and X-ray assessments, as applicable to the experimental protocol in

Manuscripts #1 and #2. This selection determined which animals underwent assessments and was distinct from random allocation to treatment groups.

Behavioral assessments of control animals and MES-stimulated animals that did not develop paralysis were performed under blind conditions. Animals developing paralysis were identified by direct visual observation to enable timely assessment; therefore, identification of paralysis itself was not blinded. Among animals that developed persistent paralysis, allocation to the 17(S)-HDHA-treated or untreated group followed a chronological alternating sequence. The first eligible animal was assigned to the 17(S)-HDHA-treated group, the second to the untreated group, and subsequent animals were assigned alternately to the two groups. Histological quantification, transcriptomic analyses, Western blotting, identification of endogenous 17(S)-HDHA in rat cerebrospinal fluid (CSF), cytokine and chemokine profiling, and serum biochemical analyses were performed by investigators blinded to experimental group for the animals included in the respective analyses. MRI and electromyographic (EMG) assessments were not performed under blinded conditions.

Humane Endpoints, Animal Monitoring, and Welfare. Animals were monitored daily for general health and well-being, including access to and the ability to consume food and water, spontaneous locomotor activity, behavioral changes, signs of pain or distress, and vaginal bleeding in pregnant rats. Monitoring also included assessment of spontaneous locomotor recovery following MES stimulation. Animals exhibiting severe or persistent distress, inability to eat or drink, or other signs of significant deterioration were to be euthanized in accordance with the approved institutional animal-care and ethics protocols. These procedures were intended to minimize animal suffering and ensure compliance with applicable animal-welfare standards.

Persistent hindlimb paralysis following MES stimulation was the principal expected experimental outcome. Pregnancy termination in eight non-paralyzed MES-stimulated animals was an additional adverse event. These animals were euthanized and excluded from subsequent analyses in accordance with the approved welfare protocol.

Housing, Husbandry, and Ethical Approval. Animal care and husbandry followed applicable institutional policies at Albert Einstein College of Medicine (New York, NY, USA), New York Medical College (Valhalla, NY, USA), Universidade de Ribeirão Preto (São Paulo, Brazil) and Universidade Federal do Rio de Janeiro (Rio de Janeiro, Brazil), together with applicable animal-welfare regulations and the *Guide for the Care and Use of Laboratory Animals*. Protocol-specific procedures, including the use of pregnant animals and awake, unanesthetized MES stimulation, were approved by the relevant institutional animal-care and ethics committees.

Pregnancy was an integral component of the experimental model. The use of awake animals avoided potential confounding effects of anesthetic agents on seizure induction and injury development. Animals were housed individually under controlled light–dark cycles and received veterinary care throughout the study.

Data Availability

The microarray dataset (Manuscript #1) is publicly available through the Gene Expression Omnibus (GEO) under accession number GSE345827. Data supporting the other findings, including histological, biochemical, X-ray, MRI, and functional data, are available from R.R. (Fiocruz) upon reasonable request. Rat cerebrospinal-fluid (CSF) lipidomics and *Alox15* data are available from K.G. (University of California, Berkeley). Rat serum biochemical measurements are available from R.O.B. (Universidade de Ribeirão Preto). Human CSF lipidomics data and measurements of deuterium-labeled 17(S)-HDHA in rats are available from F.C.S.N. (Universidade Federal do Rio de Janeiro) upon reasonable request and subject to applicable ethical and data-sharing restrictions.

Assessment of Spinal Cord Penetration Under Physiological Conditions

A cohort of nine non-pregnant rats was used to assess the SC penetration of systemically administered 17(S)-HDHA in the absence of experimentally induced injury. Animals were allocated to three groups (n = 3 per group): saline-injected controls, rats receiving deuterium-labelled 17(S)-HDHA [d_5-17(S)-HDHA], and rats receiving unlabelled 17(S)-HDHA. SC tissue was collected 45 min after intravenous administration, and tissue concentrations of the administered compounds were measured by liquid chromatography–tandem mass spectrometry (LC–MS/MS), as applicable (**Fig. 1**). This experiment was designed to determine whether circulating 17(S)-HDHA could reach SC tissue under physiological conditions, without prior ischemic disruption of the blood–spinal cord barrier.

Assessment of Treatment-Associated Metabolic Effects

A separate cohort of 18 non-pregnant rats was used to evaluate treatment-associated metabolic effects in the absence of SCI or MES stimulation. Animals were allocated to three groups (n = 6 per group): untreated controls, 17(S)-HDHA-treated rats, and methylprednisolone-treated rats. Metabolic outcomes were assessed to characterize the systemic effects of these treatments independently of those potentially associated with ischemic injury, seizure induction, or the associated systemic stress. The specific treatment regimens, metabolic endpoints, and sampling time points are detailed in the corresponding Methods and Results sections.

Tissue Collection, Histology and Immunohistochemistry. At the designated experimental endpoints (days 1 and 5 after paralysis), animals were deeply anesthetized and transcardially perfused with 150-200 mL ice-cold phosphate-buffered saline (PBS, pH 7.4), followed by 250-300 mL 4% paraformaldehyde (PFA) in PBS. SCs encompassing the entire lesion site, including segments rostral (T8) and caudal (T12) to the injury epicenter (T10), were carefully dissected, post-fixed overnight in 4% PFA at 4°C, washed in PBS, and stored in PBS at 4°C until processing. For histological analysis, SC segments were embedded in paraffin, and 10-µm transverse sections were prepared using a rotary microtome. Sections were processed for hematoxylin and eosin (H&E) staining or immunohistochemistry. For immunofluorescence, sections were incubated with the following primary antibodies: anti-glial fibrillary acidic protein (GFAP; 1:500; Invitrogen), anti-CD11b (1:1500; eBioscience), and anti-neuronal nuclei (NeuN; 1:5000; Merck Millipore). Cell nuclei were counterstained with 4′,6-

diamidino-2-phenylindole (DAPI; 1:1500; Merck Millipore). Immunoreactivity was detected using appropriate fluorophore-conjugated secondary antibodies, and images were acquired under identical microscope settings for all experimental groups.

For biochemical analyses, freshly dissected SC tissue was rapidly frozen in liquid nitrogen immediately after collection and stored at −80°C until analysis. Cerebrospinal fluid (CSF) samples were collected immediately before tissue harvesting. Animals were anesthetized with ketamine/xylazine (40/5 mg/kg, intraperitoneally), and approximately 100 µL of CSF was obtained by atlanto-occipital puncture, immediately frozen, and stored at −80°C until biochemical analysis.

Three-dimensional spinal cord reconstruction and lesion volumetry. 3D reconstruction and volumetric analyses were performed on day 5 after injury using three experimental groups: control rats (n = 5), untreated MES-paralyzed rats (n = 5), and 17(S)-HDHA-treated MES-paralyzed rats (n = 4). Approximately 300 consecutive transverse SC sections, each 10 µm thick, spanning the T8–T12 segments were collected from each animal and stained with H&E. Every twentieth section, corresponding to an interval of 200 µm, was selected for 3D reconstruction and volumetric analysis. Each selected section was inspected for processing artifacts and tissue distortion. Sections unsuitable for analysis were manually excluded, and missing data were interpolated from adjacent sections to maintain reconstruction continuity. Following assessment of tissue integrity, two investigators independently performed manual segmentation while blinded to experimental group, applying consistent segmentation criteria to delineate the SC outline, white matter, gray matter, central canal, regions of reactive gliosis, and areas of tissue vacuolization. Discrepancies between investigators were resolved through joint review and consensus before three-dimensional reconstruction and volumetric analysis.

3D reconstructions were generated using the rendering functions of Neurolucida® and Neurolucida Explorer® (version 5.05.4; MBF Bioscience, Williston, VT, USA). For untreated and 17-HDHA-treated animals, reconstructions were generated from SC levels corresponding anatomically to the lesion epicenter identified within T9–T11 in stimulated animals. Representative 3D models were generated from the averaged contours of adjacent serial sections obtained from animals within the same experimental group. Total lesion volume, calculated as the volume of SC atrophy, was determined by integrating the segmented lesion area across serial sections using the Cavalieri principle. Volumetric measurements were performed using Neurolucida Explorer®. Vacuolar degeneration was evaluated qualitatively but was not incorporated into volumetric analyses because variability in the rostrocaudal alignment of thoracic sections among animals precluded reliable comparison of individual vacuolar lesions. Group comparisons were performed using one-way analysis of variance (ANOVA) followed by Tukey–Kramer multiple-comparison post hoc testing. A two-tailed $P < 0.05$ was considered statistically significant.

Preparation of 17(S)-HDHA. The synthesis of 17(S)-HDHA involved a biogenic approach, utilizing DHA (Cayman Chemical) and soybean LOX (Type IV), along with 5-LOX from potato. Various ratios of substrate to enzyme were employed to yield specific product profiles, as previously detailed[1,2]. Following the described methodology, reactions were terminated via acidification, and subsequent extraction led to the isolation of products via RP-HPLC. For identification purposes, stringent physical criteria were established, encompassing standard HPLC retention times, specific UV chromophores, as well as major and signature ions identified through GC/MS and LC/MS analyses[1-3]. Notably, distinct standards were employed for comparison, including docosanoids such as 7S,17S-diHDHA, 14S-HDHA, 7S-HDHA, and 4S-HDHA. Despite sharing similar UV characteristics, these compounds exhibited discernible retention times in our HPLC system, ensuring clear differentiation from 17S-HDHA and NPD1.

10-15 min following the onset of paralysis, a 7 µg bolus dose of 17(S)-HDHA was IV administered into the rat's tail vein, followed by subsequent doses every other day until the 5th day post-paralysis. Each injection was freshly prepared from the 17(S)-HDHA stock solution, which was kept at -80ºC and prepared on the day of administration. The preparation process involved diluting 7 µg of 17(S)-HDHA, stored in individual Eppendorf tubes (2 mM), in 100 µl of saline at RT injected within 5-10 min of its dilution. The dose of 17(S)-HDHA was selected based on previous in vivo studies demonstrating that specialized pro-resolving mediators (SPMs) exert biological activity within the CNS following systemic administration despite an intact blood–brain barrier[3,4], as well as on previous studies evaluating SPM administration after SCI[5].

Lipid mediator analysis. For endogenous product analysis, frozen SC samples were homogenized (4˚C) in 100% MeOH containing PGB_2 (50 ng) as an internal standard for recovery and extracted by a C18 solid phase as previously detailed[6]. Methyl format fractions were taken to dryness under a gentle stream of nitrogen and resuspended in MeOH (100 µl) and stored at -80˚C.

Synthetic standards for 12-HETE, 15-HETE, 5-HETE, 17-HDHA, 14-HDHA, 7-HDHA were purchased from Cayman Chemical (Ann Arbor, MI). 17(S)-HDHA for biological assays was prepared by incubation of DHA (Caymen Chemical) and soybean LOX (Type IV, Sigma). Each reaction condition used was optimized as previously described[1,2]. Reactions were terminated by acidification, extracted and 17S-HDHA isolated by RP-HPLC using a Beckman Coulter Ultrasphere column (4.6x250 mm, 5µm, Phenomenex, Torrance, CA). Physical criteria for identification such as HPLC retention times, specific UV chromophores, as well as GC/MS and LC/MS major and signature ions have been established for 17*S*-HDHA[1-3,6]. RP-HPLC purified 17(S)-HDHA (2-4 mM stock, purity ≥ 98%) was stored in 100% ETOH at -80˚C. Endogenous arachidonic acid LOX products such as 12*S*-HETE, 15*S*-HETE, 5*S*-HETE as well as 14*S*-HDHA, 7*S*-HDHA and 4*S*-HDHA, which exhibit similar UV and MS characteristics, had distinct retention times in our HPLC system and did not coelute with 17*S*-HDHA.

Human cerebrospinal fluid lipid extraction. Cerebrospinal fluid (CSF) samples were subjected to protein precipitation followed by solid-phase extraction (SPE), based on previously established protocols for the analysis of specialized pro-resolving lipid mediators in biological fluids[7,8]. Briefly, CSF was mixed with

methanol (1:2, v/v) containing the deuterated internal standard 17(S)-HDHA-d_5 (Item No. 29797; Cayman Chemical, Ann Arbor, MI, USA) at a final concentration of 500 pg mL^{-1}. The internal standard was used to monitor lipid recovery and to provide an accurate chromatographic retention-time reference for identification of the corresponding endogenous analyte (17-HDHA) during HPLC-MS/MS analysis. The mixture was incubated at −30 °C for 30 min and centrifuged (14,000 × g, 15 min, 4 °C). The supernatant was collected and acidified to pH 3.5 with HCl.

SPE was performed using Oasis HLB cartridges (3 cc, 60 mg, 30 µm; Waters, Milford, MA, USA), preconditioned with 1 mL methanol and equilibrated with 1 mL ultrapure water (Milli-Q®). After sample loading, cartridges were washed sequentially with 1 mL ultrapure water and 1 mL *n*-hexane. Lipids were eluted with 1 mL ethyl acetate. The eluate was evaporated to dryness under a constant stream of nitrogen using a TurboVap® evaporation system (Biotage, Uppsala, Sweden) at room temperature to minimize thermal degradation of analytes. Dried extracts were reconstituted in 30 µL methanol:ultrapure water (25:75, v/v) containing 0.1% ammonium formate and transferred to HPLC-MS/MS autosampler vials.

Assessment of spinal cord penetration following systemic administration of 17-HDHA-d_5 and murine spinal cord lipid extraction

Animals were allocated to three groups (*n* = 3 per group): saline-injected controls, rats receiving deuterium-labelled 17(S)-HDHA [d_5-17(S)-HDHA], and rats receiving unlabelled 17(S)-HDHA. To determine whether systemically administered 17-HDHA and 17-HDHA-d_5 reached the SC, rats were anesthetized with inhaled sevoflurane and received an intravenous injection of either 200 ng 17-HDHA-d_5 (Item No. 29797; Cayman Chemical, Ann Arbor, MI, USA) or a mixture containing 200 ng 17-HDHA-d_5 plus 200 ng 17-HDHA (Item No. 33650; Cayman Chemical, Ann Arbor, MI, USA), suspended in 0.3 mL sterile saline (0.9% NaCl). Following 45 min of systemic circulation, animals were euthanized by decapitation. Multilevel laminectomy and durotomy were then performed for SC collection. The SC was immediately divided into three cryovials, each containing 0.5 mL methanol.

SC tissue was processed for lipid extraction using standardized tissue protocols[1]. Following mechanical dissociation, samples were homogenized by sonication (Sonics Materials VCX-130PB, Newtown, CT, USA) for 10 s while maintained on dry ice. After homogenization, tissue fractions were pooled into a single tube. Protein precipitation was achieved by incubation at −30 °C for 30 min followed by centrifugation (14,000 × g, 15 min, 4 °C). The residual pellet was re-extracted with 1 mL methanol under identical centrifugation conditions, and both supernatants were combined.

The pooled extract was acidified to pH 3.5 with HCl and subjected to SPE using Oasis HLB cartridges (3 cc, 60 mg, 30 µm; Waters), following the same washing and elution procedure described for CSF samples. The eluate was evaporated to dryness under nitrogen at room temperature using the TurboVap® system. Samples were reconstituted in 30 µL methanol:ultrapure water (25:75, v/v)

containing 0.1% ammonium formate and transferred to HPLC-MS/MS autosampler vials.

High-performance liquid chromatography–tandem mass spectrometry (LC-MS/MS)

Chromatographic separation and lipid mediator identification were performed using a high-performance liquid chromatography (LC) system coupled to a TSQ Quantiva triple quadrupole mass spectrometer (Thermo Fisher Scientific, Waltham, MA, USA), operating under conditions adapted from previously published methods[1]. Lipid mediators were separated on a reverse-phase C18 column (2.1 × 50 mm, 1.8 µm particle size; Agilent Technologies, Santa Clara, CA, USA) maintained at 50 °C. Gradient elution was performed using Mobile Phase A (ultrapure water supplemented with ammonium formate and ammonium hydroxide) and Mobile Phase B (100% methanol).

For CSF extracts, the chromatographic gradient consisted of 50% B (0–1.0 min), a linear increase to 80% B (1.0–5.0 min), a linear increase to 98% B (5.0–8.5 min), followed by a rapid return to 50% B (8.5–8.6 min) and column re-equilibration until 11.0 min. The flow rate was maintained at 0.4 mL min^{-1}, and the injection volume was 5 µL.

For SC extracts, the gradient consisted of 10% B (0–1.0 min), a linear increase to 25% B (1.0–2.0 min), followed by an increase to 70% B (2.0–2.1 min) maintained until 9.0 min, an increase to 100% B (9.0–9.1 min) maintained until 13.0 min, and a return to the initial conditions (10% B) at 13.1 min, followed by re-equilibration until 14.0 min. The flow rate was 0.3 mL min^{-1}, and the injection volume was 5 µL. The TSQ Quantiva mass spectrometer was equipped with a heated electrospray ionization (HESI) source operating in negative ion mode (ESI−). Source parameters were as follows: spray voltage, 2.5 kV; ion transfer capillary temperature, 300 °C; and vaporizer temperature, 350 °C.

Data acquisition was performed in multiple reaction monitoring (MRM) mode. Identification of endogenous 17-HDHA and the deuterated internal standard (17-HDHA-d_5) was confirmed by chromatographic co-elution with their respective standards at identical mean retention times (RT = 4.05 min for CSF samples and RT = 4.20 min for SC extracts). For endogenous 17-HDHA, the precursor ion *m/z* 343.3 was monitored. Quantification was based on the primary transition to fragment ion *m/z* 281.2, whereas fragment ions *m/z* 299.2 and *m/z* 329.7 were monitored as qualifier transitions for structural confirmation. For 17-HDHA-d_5, the precursor ion *m/z* 348.3 and the transition to fragment ion *m/z* 286.2 were monitored. Collision energies ranged from 12 to 15 eV and were individually optimized for each transition. Data acquisition and processing were performed using Xcalibur version 2.2 software (Thermo Fisher Scientific).

Hindlimb vector electromyographic (VEMG) recordings. Intramuscular vector electromyography (VEMG) was performed to assess the functional organization of spinal motor unit recruitment in uninjured control, vehicle-treated, and 17(S)-HDHA-treated rats. Recordings were obtained using a specially manufactured 25-gauge quadrifilar needle electrode (Delsys Inc., Boston, MA) inserted into the hindlimb musculature. The quadrifilar electrode consists of four recording

surfaces arranged within the needle cannula, allowing simultaneous acquisition of multiple differential signals. Detectors were connected intra-cannula to external EMG amplifiers in differential-pair configurations (vertical, horizontal, and diagonal), generating a three-dimensional representation of the myoelectric activity within the recording volume surrounding the electrode. Motor unit action potentials were identified by vector electromyographic analysis and Precision Decomposition, which discriminates individual motor units by interpreting vector signatures generated across two independent dipoles as distinct motor unit events, resulting depolarization of muscle fibers (MU1 and MU2), enabling characterization of motor unit recruitment and discharge behavior, as previously described[9,10].

Quadrifilar VEMG was performed in a total of six animals (n = 2 per experimental group). Each animal underwent two to three independent recordings to verify the reproducibility of the electrophysiological findings. Because repeated recordings obtained from the same animal are not statistically independent, the animal was considered the experimental unit. Accordingly, VEMG was incorporated as a physiological assessment of spinal motor circuit organization to complement the behavioral, histopathological, and molecular analyses, rather than as a primary quantitative efficacy endpoint.

SUPPLEMENTARY REFERENCES

1. Hong, S., Gronert, K., Devchand, P. R., Moussignac, R.-L. & Serhan, C. N. Novel docosatrienes and 17S-resolvins generated from docosahexaenoic acid in murine brain, human blood, and glial cells. *J. Biol. Chem.* **278**, 14677–14687 (2003).
2. Serhan, C. N. *et al.* Resolvins: a family of bioactive products of omega-3 fatty acid transformation circuits initiated by aspirin treatment that counter proinflammation signals. *J. Exp. Med.* **196**, 1025–1037 (2002).
3. Marcheselli, V. L. *et al.* Novel docosanoids inhibit brain ischemia-reperfusion-mediated leukocyte infiltration and pro-inflammatory gene expression. *J. Biol. Chem.* **278**, 43807–43817 (2003).
4. Svensson, C. I., Zattoni, M. & Serhan, C. N. Lipoxins and aspirin-triggered lipoxin inhibit inflammatory pain processing. *J. Exp. Med.* **204**, 245–252 (2007).
5. Francos-Quijorna, I. *et al.* Maresin 1 promotes inflammatory resolution, neuroprotection and functional neurological recovery after spinal cord injury. *J. Neurosci.* **37**, 11731–11743 (2017).
6. Gronert, K., Maheshwari, N., Khan, N., Hassan, I. R., Dunn, M. & Schwartzman, M. L. A role for the mouse 12/15-lipoxygenase pathway in promoting epithelial wound healing and host defense. *J. Biol. Chem.* **280**, 15267–15278 (2005).
7. Dalli J, Colas RA, Walker ME & Serhan CN. Lipid mediator metabolomics via LC-MS/MS profiling and analysis. *Methods Mol. Biol.* **1730**, 59–72 (2018).
8. English JT, Norris PC, Hodges RR, Dartt DA & Serhan CN. Identification and profiling of specialized pro-resolving mediators in human tears by lipid mediator metabolomics. *Prostaglandins Leukot. Essent. Fatty Acids* **117**, 17–27 (2017).

9. De Luca, C. J., Gonzalez-Cueto, J. A., Bonato, P. & Adam, A. Motor unit recruitment and proprioceptive feedback decrease the common drive. *J. Neurophysiol.* **101**, 1620–1628 (2009).
10. Roark, R. M., Li, J. C., Schaefer, S. D., Adam, A. & De Luca, C. J. Multiple motor unit recordings of laryngeal muscles: the technique of vector laryngeal electromyography. *Laryngoscope* **112**, 2196–2203 (2002).
11. Serhan, C. N. & Savill, J. Resolution of inflammation: the beginning programs the end. *Nat. Immunol.* **6**, 1191–1197 (2005).
12. Serhan, C. N., Gotlinger, K., Hong, S., Lu, Y., Siegelman, J., Baer, T., Yang, R., Colgan, S. P. & Petasis, N. A. Anti-inflammatory actions of neuroprotectin D1/protectin D1 and its natural stereoisomers: assignments of dihydroxy-containing docosatrienes. *J. Immunol.* **176**, 1848–1859 (2006).

SUPPLEMENTARY FIGURES

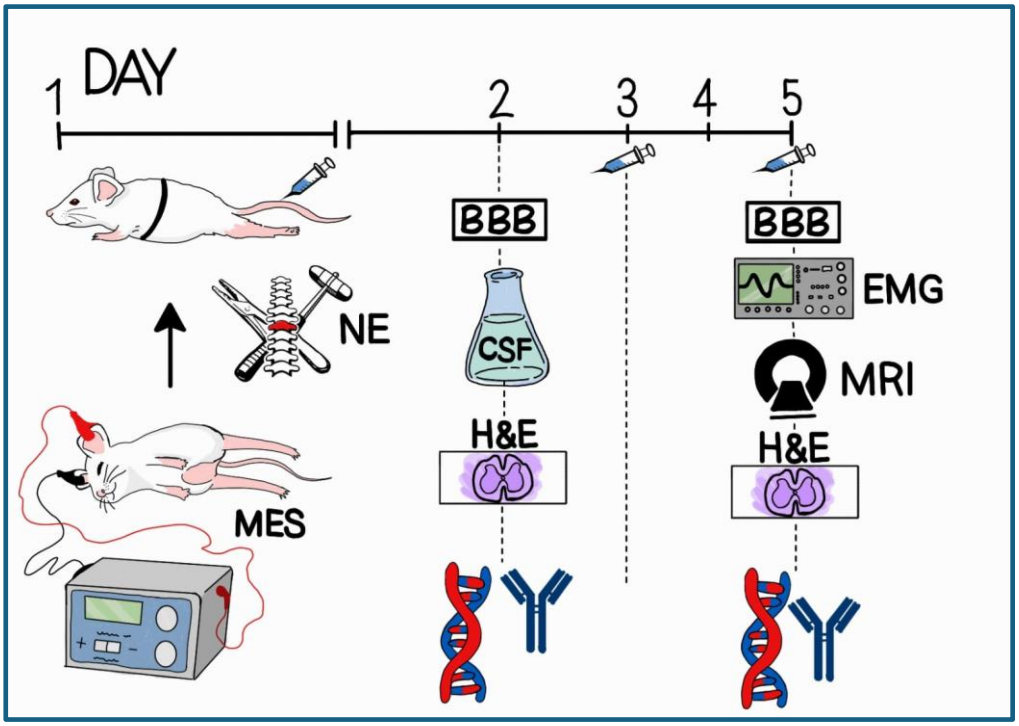

Fig. S1. Experimental design and treatment paradigm.

Adult Sprague–Dawley rats underwent ischemic SCI induced by the repeated transauricular maximal electroshock seizure (**MES**) paradigm (120 V, 50 Hz, 2 s; see Methods and the companion manuscript for details). Immediately after the onset of irreversible hindlimb paralysis (day 1), animals underwent neurological examination (**NE**), including assessment of nociceptive responses to standardized mechanical pinches applied to the hindlimbs, tail, and trunk to determine the neurological level of injury (**black circle**). Animals subsequently received an intravenous injection of either vehicle or 17(S)-HDHA, followed by additional injections on days 3 and 5, for a total of three administrations over the 5-day experimental period. A subgroup of animals was euthanized 24 h after paralysis onset for mechanistic studies. Cerebrospinal fluid (**CSF**) was collected for targeted lipidomic analysis, and spinal cord (**SC**) tissue encompassing the lesion epicenter (T10) and adjacent segments (T8–T12) was harvested for transcriptomic analyses (gene expression, microarray and RT–qPCR), protein analyses (proteomics and Western blotting), lipidomics, and histopathological evaluation (**H&E**). Functional recovery was assessed using the Basso, Beattie, and Bresnahan (**BBB**) locomotor rating scale on days 2 and 5 after paralysis. At day 5, animals underwent magnetic resonance imaging (**MRI**) and electromyographic (**EMG**) recordings before tissue collection. SC samples were subsequently processed for histopathology, immunohistochemistry, and three-dimensional lesion reconstruction to quantify lesion volume, tissue preservation, neuronal survival, astrocytic responses, and inflammatory cell infiltration. The **DNA double-helix icon** denotes transcriptomic analyses, whereas the **antibody** (**Y-shaped**) **icon** denotes protein analyses and Western blotting.

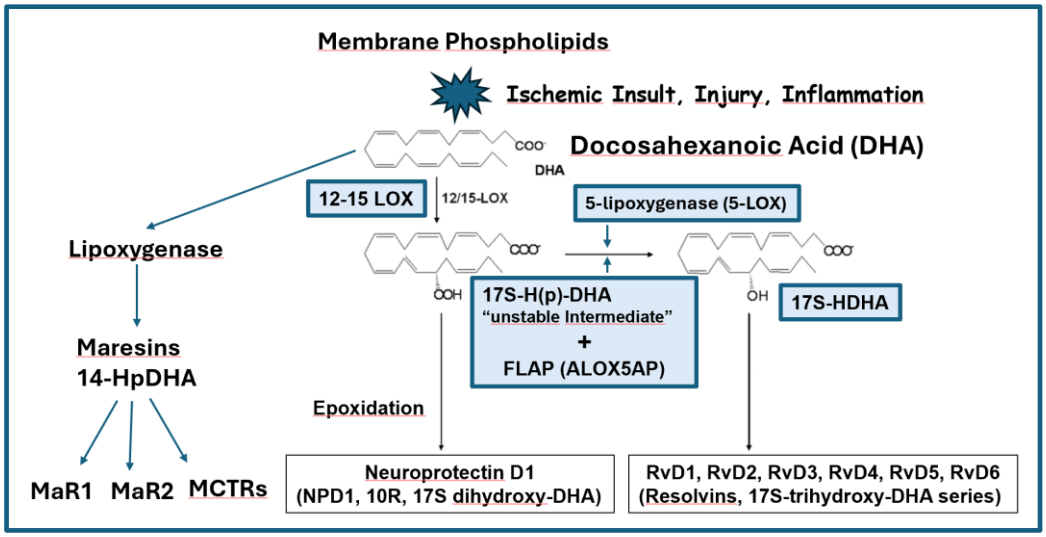

Fig. S2. Biosynthetic pathways downstream of ALOX15 and endogenous production of 17(S)-HDHA after ischemic spinal cord injury.

The schematic illustrates the principal docosahexaenoic acid (DHA)-derived lipid mediator pathways initiated by arachidonate 15-lipoxygenase (ALOX15, 12/15-LOX). Oxidation of DHA by ALOX15 generates the unstable intermediate 17S-hydroperoxy-docosahexaenoic acid (17S-HpDHA), which is subsequently reduced to 17S-hydroxydocosahexaenoic acid (17S-HDHA) or enzymatically converted to neuroprotectin D1 (NPD1). In the presence of 5-lipoxygenase (5-LOX), 17S-HDHA serves as the precursor for D-series resolvins (RvD1–RvD6), whereas an alternative ALOX15-dependent pathway generates 14S-HDHA, the precursor of maresins (MaR1 and MaR2) and maresin conjugates in tissue regeneration (MCTRs). The 5-lipoxygenase-activating protein (FLAP; ALOX5AP) functions as an essential accessory protein by presenting substrate to 5-LOX and facilitating leukocyte lipid mediator[1,11,12]. Despite activation of the ALOX15 pathway after ischemic SCI, targeted lipidomic analyses of SC tissue and cerebrospinal fluid (CSF) detected endogenous formation of 17S-HDHA only. Neither 14S-HDHA nor downstream specialized pro-resolving mediators, including NPD1, D-series resolvins, maresins, or MCTRs, were detected during the hyperacute phase (24 h) after injury. Notably, endogenous 17S-HDHA was identified in the CSF of both paralyzed rats and patients with SCI, supporting its translational relevance and identifying 17S-HDHA as the predominant DHA-derived lipid mediator generated during the earliest response to ischemic SCI.

PARAMETERS	*Control (n=6)*	*17(S)-HDHA (n=6)*	*Metilprednisolona (n=6)*
Glicemia (mg/dL)	**151 ± 8.8**	**145 ± 9.7***	**184 ± 10***
Na^+ (mmol/L)	**133 ± 4.3**	**140 ± 1.1**	**140 ± 1.7**
K^+ (mmol/L)	**4.13 ± 0.9**	**4.7 ± 0.5**	**4.56 ± 0.3**
Ca^{2+} (mmol/L)	**11.18 ± 0.9**	**12.15 ± 0.6**	**12.65 ± 0.5**
Mg^{2+} (mg/dL)	**2.36 ± 0.13**	**2.51 ± 0.1**	**2.55 ± 0.1**

SI Table 1. Acute systemic metabolic effects of intravenous 17(S)-HDHA and methylprednisolone.

Serum biochemical analyses were performed 24 h after a single intravenous administration of vehicle, 17(S)-HDHA, or methylprednisolone to evaluate potential systemic metabolic effects. Animals treated with 17(S)-HDHA remained normoglycemic, exhibiting serum glucose concentrations comparable to those of vehicle-treated controls, whereas methylprednisolone significantly increased blood glucose levels. Serum electrolyte concentrations (Na^+, K^+, Ca^{2+}, and Mg^{2+}) were not significantly different among the experimental groups, indicating that neither treatment altered systemic electrolyte homeostasis during the study period. A total of 18 adult female rats were studied (n = 6 per group). Data are presented as mean ± SD. Statistical analyses were performed using one-way ANOVA followed by the appropriate post hoc multiple-comparison test. $P < 0.05$ versus vehicle-treated controls.